DLL1- and DLL4-Mediated Notch Signaling Is Essential for Adult Pancreatic Islet Homeostasis

Marina Rubey,[1,2] Nirav Florian Chhabra,[1,2] Daniel Gradinger,[1,2] Adrián Sanz-Moreno,[1] Heiko Lickert,[2,3,4] Gerhard K.H. Przemeck,[1,2] and Martin Hrabě de Angelis[1,2,5]

Diabetes 2020;69:915–926 | https://doi.org/10.2337/db19-0795

Genes of the Notch signaling pathway are expressed in different cell types and organs at different time points during embryonic development and adulthood. The Notch ligand Delta-like 1 (DLL1) controls the decision between endocrine and exocrine fates of multipotent progenitors in the developing pancreas, and loss of *Dll1* leads to premature endocrine differentiation. However, the role of Delta-Notch signaling in adult tissue homeostasis is not well understood. Here, we describe the spatial expression pattern of Notch pathway components in adult murine pancreatic islets and show that DLL1 and DLL4 are specifically expressed in β-cells, whereas JAGGED1 is expressed in α-cells. We show that mice lacking both DLL1 and DLL4 in adult β-cells display improved glucose tolerance, increased glucose-stimulated insulin secretion, and hyperglucagonemia. In contrast, overexpression of the intracellular domain of DLL1 in adult murine pancreatic β-cells results in impaired glucose tolerance and reduced insulin secretion, both in vitro and in vivo. These results suggest that Notch ligands play specific roles in the adult pancreas and highlight a novel function of the Delta/Notch pathway in β-cell insulin secretion.

Diabetes is a major metabolic disease with over 400 million people diagnosed and a large number of undiagnosed adults (1). Genome-wide association studies have implicated a large number of genes in the pathology of this disorder (2). Among these, the Delta/Notch (D/N) pathway components *Dll4* and *Notch2* were found to be associated with type 2 diabetes (3), sparking investigation into their roles in glucose metabolism. The highly conserved D/N signaling pathway is crucial for embryonic development in a wide range of different tissues (4). Although Notch activity is required during pancreatic development (5), some D/N components have also been reported to be active during adulthood. D/N signaling mediates cell-cycle regulation via transmembrane-bound ligands (DLL1, DLL3, DLL4, JAGGED1, and JAGGED2) and receptors (NOTCH1–4). Studies have shown that DLL1 and DLL4 regulate tissue renewal and maintain intestinal progenitor cells (6). Furthermore, NOTCH/NEUROG3 signaling is active in adult rodent and human pancreatic islets (7). Two recent studies gave new insights into the regulation of β-cell function by NOTCH1 and DLL4 in adult mouse islets (8,9). Whereas NOTCH1 is reported to regulate β-cell maturation and proliferation (8), DLL4 is associated with regulation of islet function (9). To date, however, no comprehensive analysis of D/N pathway components has been performed in the adult pancreas.

Ligand binding to Notch receptors leads to proteolytic cleavages that, in turn, release the Notch-intracellular domain, which enters the nucleus and acts with cofactors as a transcriptional regulator (10,11). Interestingly, the ligands also undergo proteolytic cleavage and release their intracellular domains, which can also enter the nucleus (12,13). However, their precise function is poorly understood (14,15). Moreover, the location and possible function of other D/N pathway components in the adult pancreas

[1]Institute of Experimental Genetics and German Mouse Clinic, Helmholtz Zentrum München, Neuherberg, Germany
[2]German Center for Diabetes Research, Neuherberg, Germany
[3]Institute of Diabetes and Regeneration Research and Institute of Stem Cell Research, Helmholtz Zentrum München, Neuherberg, Germany
[4]Medical Faculty, Technische Universität München, Munich, Germany
[5]Centre of Life and Food Sciences, Weihenstephan, Technische Universität München, Freising, Germany

Corresponding author: Martin Hrabě de Angelis, hrabe@helmholtz-muenchen.de

Received 21 August 2019 and accepted 22 January 2020

This article contains Supplementary Data online at https://diabetes.diabetesjournals.org/lookup/suppl/doi:10.2337/db19-0795/-/DC1.

M.R. and N.F.C. contributed equally.

M.R. is currently affiliated with WMC Healthcare GmbH, Munich, Germany.

D.G. is currently affiliated with PSI CRO AG, Munich, Germany.

have yet to be determined. Considering that dysfunctional pancreatic β-cells are a major characteristic of type 2 diabetes (16), detailed studies of the D/N signaling pathway are required.

Here, we provide a broad expression analysis of selected D/N pathway components in the mouse adult pancreas and report the presence of cell type–specific protein expression. Furthermore, we show that ligands DLL1 and DLL4 are active and play a role in β-cell insulin secretion by utilizing conditional β-cell–specific mouse models. Finally, we report the presence of the DLL1 intracellular domain (DICD) in adult β-cells and describe a possible function.

RESEARCH DESIGN AND METHODS

Generation of Transgenic Mice

Mice carrying floxed alleles for both *Dll1* (17) and *Dll4* (18) (background Sv/129.C57BL/6 × C57BL/6J) were intercrossed with Pdx1-Cre^{ERT} (19) (C3HeB/FeJ) mice. *Cre*$^{+}$ heterozygous F1 offspring were intercrossed to acquire homozygous animals for *Dll1*, *Dll4*, or both in F2. Homozygous mice with the same genetic background (Dll1$^{+/+}$Dll4$^{+/+}$, Dll1$^{lox/lox}$Dll4$^{+/+}$, Dll1$^{+/+}$Dll4$^{lox/lox}$, or Dll1$^{lox/lox}$Dll4$^{lox/lox}$) were used to create β-cell-specific homozygous lines lacking either *Dll1* (β-DLL1) or *Dll4* (β-DLL4) or both simultaneously (β-D1D4). *Cre*$^{+}$ wild-type littermates were used as controls.

To generate a mouse model with overexpression of the DICD, we used gene targeting into the endogenous *Rosa26* locus by recombinase-mediated cassette exchange (RMCE) (20). The cDNA sequence of DICD and the coding sequence of the fluorescent reporter IRES-VENUS cassette were cloned independently from each other into two TOPO TA Vectors (pENTRY Clones). Subsequently, DICD and the reporter cassette were joined via homolog end-joining into a target vector (pEx-CAG-ROSA26), thus generating the pRMCE-DICD-IRES-VENUS donor vector (Supplementary Fig. 1*A*). To enable RMCE in vivo, the ΦC31/attP integrase–mediated recombination approach (21) was used in IDG3.2 ROSA26 acceptor embryonic stem (ES) cells, which have a mixed C57BL6/J-129S6/SvEvTac genetic background (22). To avoid the influence of the neomycin resistance cassette on genes near the target locus *Rosa26*, the pgk promoter and the neo-bpA cassette were removed by flippase-mediated removal. Successfully recombined ES cells were selected and used for blastocyst injection. Chimeric mice were mated with C57BL/6J wild-type mice to obtain germline transmission. The new mouse line was named Rosa26-DICD and outcrossed to C3HeB/FeJ wild-type mice for five generations.

The expression of the DICD-IRES-VENUS construct was driven by the *Cre*-mediated excision of the floxed puro-polyA stop cassette (Supplementary Fig. 1*B*). To specifically induce DICD expression in adult β-cells, Rosa26-DICD mice were intercrossed with Pdx1-Cre^{ERT} mice (19) and maintained on a C3HeB/FeJ background.

For all models, *Cre*-dependent recombination was activated in weaned offspring by feeding tamoxifen-containing chow (Genobius; 400 mg/kg) for 4 weeks. Genotyping was done by PCR with specific primers, as listed in Supplementary Table 1. All experimental procedures were performed in accordance with German and European Union guidelines. All mice were housed in specific pathogen-free conditions with a 12-h light/dark cycle and free access to food (standard chow diet, 1328 – Hybridpellet; Altromin) and water.

Tissue Preparation and Immunohistochemistry

Mice were sacrificed by cervical dislocation, and the pancreata were excised, fixed in 4% paraformaldehyde-PBS for 20 min, and then washed in PBS for 5 min followed by serial incubations in 9% and 15% sucrose solutions for 1 h each and overnight in 30% solution. Thereafter, pancreatic tissue was embedded in O.C.T. solution (Thermo Fisher Scientific) and frozen; 9-μm sections were cut using a Leica CM1850 Cryostat (Leica Microsystems), and three sections were placed each on a Superfrost Plus slide (Menzel-Gläser), maintaining >100 μm of distance between each slide. All antibodies used are described in Supplementary Tables 2 and 3. Sections were blocked with 5% BSA in PBS with Tween 20 and subsequently incubated with appropriate primary antibodies overnight at 4°C. After washing, slides were incubated in suitable secondary antibodies at room temperature for 90 min. Finally, sections were washed and covered with VECTASHIELD mounting medium (Vector Laboratories). Whole-slide images were acquired using a Nanozoomer (Hamamatsu) and analyzed using NDP.view 2 software (Hamamatsu). A cell counter application on ImageJ software was used for counting and quantification of insulin-, glucagon-, Ki-67–, and MAFB-positive cells. A minimum of 120 islets or 3,000 cells were counted per genotype. Final images were acquired using a Leica TCS SP5 confocal microscope.

Intraperitoneal Glucose Tolerance Test

Mice were fasted overnight for 16 h. Weight and basal blood levels were measured before an intraperitoneal administration of 2 g/kg glucose (Braun). Blood glucose levels were measured at 5, 15, 30, 60, and 120 min after glucose administration, and plasma was collected at 0, 15, and 30 min.

In Vitro Stimulatory Studies and Immunocytochemistry

Islets were isolated from mice and maintained as described previously (23). Isolated islets were incubated with 1.5 mmol/L glucose in Krebs-Ringer buffer for 2 h. Next, islets (10/mouse/experiment) were stimulated for 2 h at 37°C with different glucose concentrations along with 2.5 μmol/L Forskolin (Sigma-Aldrich), 10 μmol/L norepinephrine (Sigma-Aldrich), 10 μmol/L ESI-09 (Biozol), 30 mmol/L KCl (Sigma-Aldrich), and 100 nmol/L Exendin-4 (Sigma-Aldrich) in combination with 16.7 mmol/L glucose. To assess the whole-islet protein content, unstimulated islets (10/mouse) were taken and dissolved in acid ethanol. For immunocytochemistry, islets were dispersed in 0.05% Trypsin-EDTA (Sigma-Aldrich) for 5 min and allowed to settle on slides coated with Cell-Tak (Corning) in serum-free medium for 1 h. Cells were then fixed in 4%

paraformaldehyde-PBS for 10 min at room temperature and permeabilized in 0.3% Triton X-100 for 15 min. Next, cells were blocked in 10% horse serum and incubated with primary antibodies for 2 h and with secondary antibodies for 45 min. Images were acquired using an Axio Imager M2 microscope (Zeiss) and were analyzed (~3,000 cells per mouse) with QuPath (24) software version 0.1.2.

RNA Isolation, cDNA Synthesis, and Quantitative Real-time PCR

Islet RNA isolation was performed with the RNeasy Plus Micro Kit (QIAGEN) according to the manufacturer's instructions. Quantitative RT-PCR (qRT-PCR) was used for amplification of cDNA samples, using the LightCycler 480 DNA SYBR Green I Master (Roche) with primers listed in Supplementary Table 1. Crossing point (Cp) values were obtained with the automatic Cp analysis of the LightCycler 480 software (Roche) using the second derivative maximum method. All subsequent data analyses were performed in Microsoft Excel. The results were determined using the equations outlined in the geNorm 3.5 user manual, which are mathematically identical to the $2-\Delta\Delta$Cp method (25).

Hormone Assays

Insulin and glucagon obtained from in vitro stimulatory studies and plasma samples were analyzed using the Mercodia Mouse Insulin ELISA kit and Mouse Glucagon ELISA kit according to the manufacturer's instructions.

Statistics

Statistical analysis was achieved using GraphPad Prism software and applied using heteroscedastic two-tailed Student *t* test and one-way or two-way ANOVA with Bonferroni post hoc test for multiple comparisons. A value of $P < 0.05$ was considered significant. Unless stated otherwise, all results are described as mean ± SD.

Data and Resource Availability

All data generated or analyzed during the current study are included in the published article and Supplementary Data.

RESULTS

Expression of D/N Pathway Components in the Adult Murine Pancreas

To analyze the expression of Notch receptors and ligands in adult pancreatic islets, we used qRT-PCR analysis in wild-type C3HeB/FeJ mice. We found that the *Notch1* and *Notch2* genes, Notch ligand genes *Jag2* and *Dll4*, and Notch target genes *Hes1* and *Hes6* were strongly expressed and at comparable levels, followed by the Notch ligand genes *Jag1 and Dll1* (Fig. 1*A*). Minimal expression was detected for *Notch3* and *Notch4* as well as for the target genes *Hey1* and *Hey2* (Fig. 1*A*), indicating differential expression of D/N components in adult islets. To visualize and quantify the islet cell type–specific expression pattern, we used ligand- and receptor-specific antibodies along with markers for α-, β-, and δ-cells, and performed coimmunostainings on pancreatic sections and on dispersed islet cell types. Although NOTCH1 expression was found in most α-, β-, and δ-cells, NOTCH2 and NOTCH4 showed limited expression, with a small population (8%) of δ-cells expressing the former and that of β-cells (15%) expressing the latter (Fig. 1*B* and Supplementary Fig. 2). Interestingly, NOTCH3 expression was not detected in any islet cell type (Fig. 1*B* and Supplementary Fig. 2). Similarly, JAGGED2, although it has high mRNA expression, was not detectable in the islets, while expression of JAGGED1 was abundantly found in islets, with ~70% of α-cells expressing the ligand (Fig. 2 and Supplementary Fig. 2). Conversely, DLL1 and DLL4 were found in most β-cells (~90%), while they had limited expression in α- and δ-cells (Fig. 2 and Supplementary Fig. 2). These results demonstrate that D/N pathway components have a broad and heterogeneous expression pattern in adult mouse islets, such as DLL1 and DLL4 expression in β-cells, strongly indicating functional relevance in a cell type–specific manner.

Dll1 and *Dll4* Are Essential for Normal Glucose Homeostasis

Since in the adult mouse pancreas DLL1 and DLL4 are predominantly expressed in β-cells, we hypothesized that active Notch signaling either maintains β-cell homeostasis or is important for β-cell function. To test this idea, we generated different β-cell–specific homozygous knockout models for *Dll1*, *Dll4*, and both genes simultaneously (see Supplementary Fig. 3*A* and *B* for breeding schemes). Since female mice are often protected from a diabetic phenotype (26) and for better comparison with other studies (8,9), only male mice were used in this study. After tamoxifen treatment, *Cre* expression was found specifically in islets (Supplementary Fig. 3*C*) along with a substantial decrease in *Dll1* and *Dll4* mRNA (Supplementary Fig. 3*D*), as well as a comparable decrease in protein expression (Supplementary Fig. 3*E*). Three mutant mouse lines (β-DLL1, β-DLL4, and β-D1D4) and control mice were investigated for body weight and blood glucose levels in an ad libitum fed state. β-DLL1 mice showed significantly increased blood glucose levels as compared with control mice (Fig. 3*B*). Body weight and blood glucose levels were not altered in β-DLL4 mice (Fig. 3*A* and *B*). However, knocking out both ligands in β-D1D4 mice resulted in significantly reduced blood glucose levels but unchanged body weight as compared with controls (Fig. 3*B*).

Because of differences in blood glucose levels between the groups, we wondered whether β-cell function was affected, especially in β-D1D4 mice. Therefore, we performed intraperitoneal glucose tolerance tests (IPGTTs) to investigate glucose disposal. Compared with controls, β-DLL1 mice showed a significant but mild decrease in glucose tolerance accompanied by a significant reduction in insulin secretion (Supplementary Fig. 4*A*), whereas β-DLL4 mice displayed a significant but modest increase in glucose tolerance with no major changes in insulin secretion (Supplementary Fig. 4*A*). In β-D1D4 mice, we noticed a clear improvement in glucose tolerance (Fig. 3*C*) resulting in

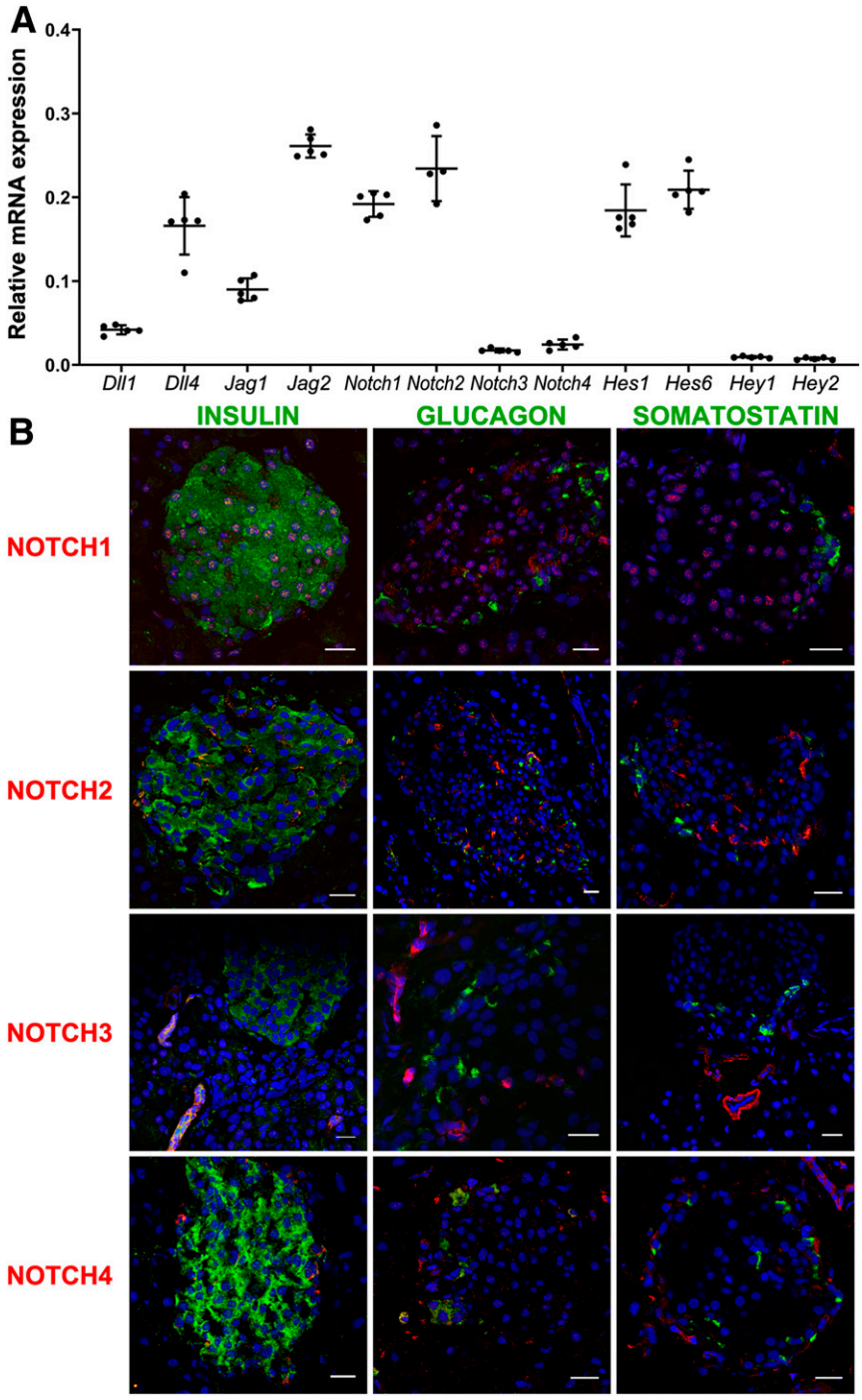

Figure 1—Expression of Notch receptors in the adult pancreas. *A*: qRT-PCR analysis of D/N components in isolated islets from 8-week-old male C3HeB/FeJ mice normalized to the housekeeping genes *Sdha* and *Ubc*; $n = 5$ (*Notch2*, $n = 4$). Data are shown as mean ± SD. *B*: Coimmunostaining of Notch receptors NOTCH1, NOTCH2, NOTCH3, and NOTCH4 with β-cell (insulin), α-cell (glucagon), and δ-cell (somatostatin) markers on pancreatic sections from 13-week-old male C3HeB/FeJ mice; $n = 3$. Nuclei were counterstained with DAPI (blue). The scale bar represents 20 μm.

a twofold increase in acute insulin response within the first 15 min (Fig. 3*D* and *E*). Ad libitum fed plasma insulin levels were unchanged in β-D1D4 mice compared with controls (Fig. 3*F*), as were the mRNA levels in isolated islets of both insulin gene isoforms (Fig. 3*G*), which was similar to the observations made for β-DLL1 and β-DLL4 islets (Supplementary Fig. 4*B*).

To confirm whether the loss of DLL1 and DLL4 leads to abnormal insulin secretion, we analyzed β-D1D4 mice in a glucose-stimulated insulin secretion assay using isolated islets. Compared with controls, basal insulin secretion at low glucose concentration (2.8 mmol/L) was not altered. However, at high glucose concentration (16.7 mmol/L), we

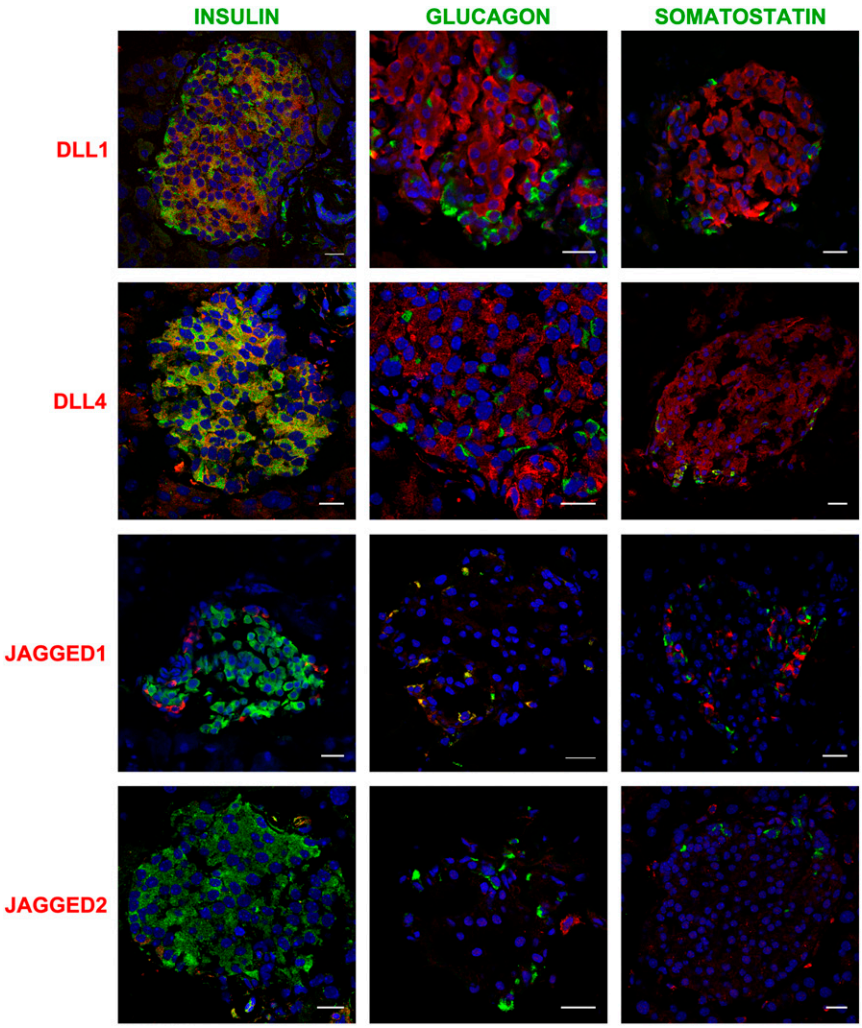

Figure 2—Expression of Notch ligands in the adult pancreas. Coimmunostaining of DLL1, DLL4, JAGGED1, and JAGGED2 with β-cell (insulin), α-cell (glucagon), and δ-cell (somatostatin) markers on pancreatic sections from 13-week-old male C3HeB/FeJ mice; $n = 3$. Nuclei were counterstained with DAPI (blue). The scale bar represents 20 μm.

observed a fourfold increase in insulin secretion (Fig. 3*H*). This was further potentiated upon stimulation with forskolin. By adding norepinephrine, which hyperpolarizes the cell and inhibits adenylyl cyclase (27), the increase in insulin secretion under high glucose conditions was normalized. Also, the addition of ESI-09, which inhibits EPAC2, a downstream target of adenylyl cyclase (28), normalized insulin secretion under high glucose conditions (Fig. 3*H*). Therefore, the concomitant loss of DLL1 and DLL4 in adult pancreatic β-cells leads to enhanced glucose clearance due to an increase in insulin secretion.

Loss of *Dll1* and *Dll4* Leads to Overproduction of α-Cells and Hyperglucagonemia

To understand whether the lack of Delta ligands leads to changes in the islet transcriptome, we carried out qRT-PCR to analyze gene expression of D/N pathway intermediates. Compared with control islets, the expression of Notch and Jagged components in β-DLL1 and β-DLL4 islets was largely unaffected with the exception of *Jag2* in islets of β-DLL1 mice (Supplementary Fig. 5*A* and *B*). Interestingly, β-D1D4 islets showed an upregulation of the α-cell–specific ligand *Jag1*, as well as a significant increase in the expression of *Notch1*, *Notch2*, and *Notch4*, and the downstream target *Hes1* (Supplementary Fig. 5*C*). Next, immunohistochemical analysis of insulin and glucagon double-stained pancreas did not reveal major differences in glucagon- and insulin-positive cells in β-DLL1 and β-DLL4 mutants compared with control mice (Fig. 4*A–C* and Supplementary Fig. 5*D*). However, significantly increased glucagon-positive staining was observed within β-D1D4 islets (Fig. 4*D* and Supplementary Fig. 5*E*). Consistent with this observation, no change was found in the insulin content of freshly isolated islets between the groups (Fig. 4*E*), whereas there was a significant increase in glucagon protein content in islets (Fig. 4*F*) and plasma (Supplementary Fig. 5*F*) from β-D1D4 mutants as compared with controls. To determine whether an increase in glucagon-positive α-cells

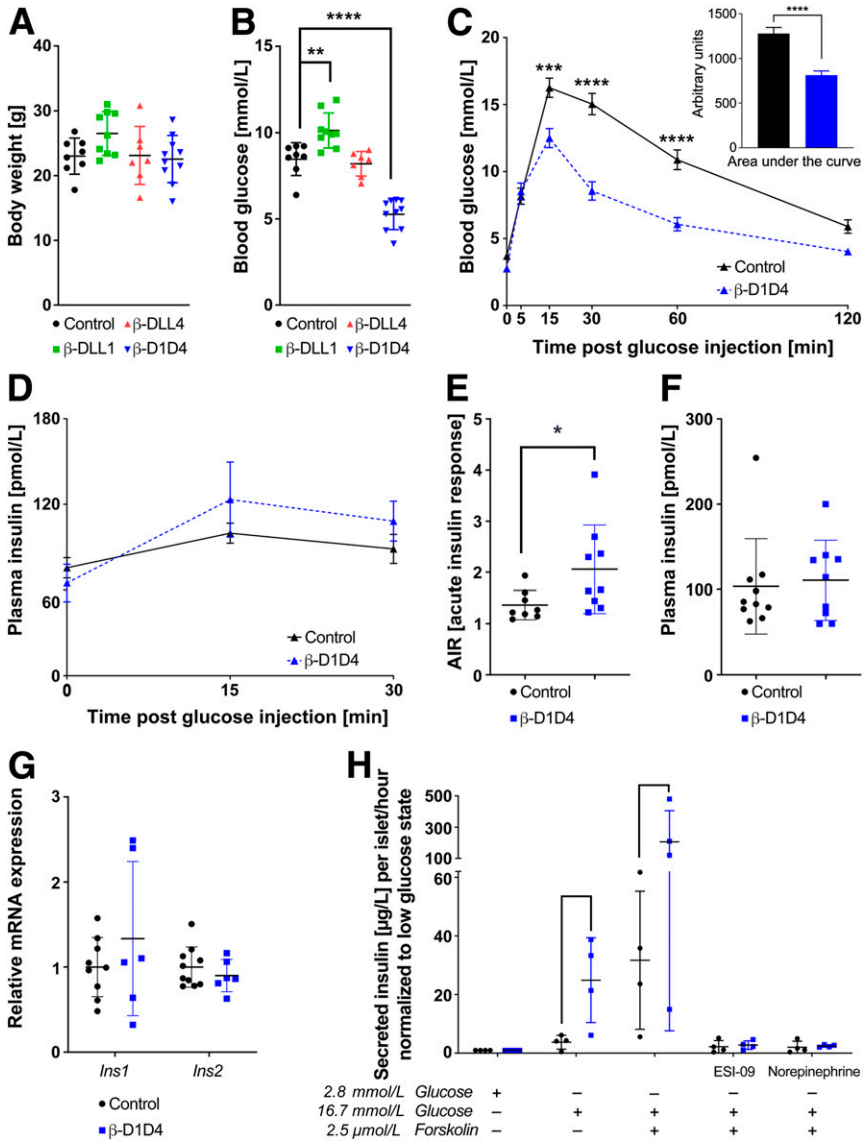

Figure 3—Glucose homeostasis in β-DLL1, β-DLL4, and β-D1D4 mice. *A*: Average ad libitum fed body weight levels. *B*: Average blood glucose levels; control $n = 8$, β-DLL1 $n = 9$, β-DLL4 $n = 7$, and β-D1D4 $n = 10$. *C*: IPGTT; control $n = 16$ and β-D1D4 $n = 18$. *D*: Plasma insulin levels during IPGTT between $t = 0$ min and $t = 30$ min. *E*: Acute insulin response during IPGTT between $t = 0$ min and $t = 15$ min; control $n = 8$ and β-D1D4 $n = 9$. *F*: Plasma insulin levels in ad libitum fed state; control $n = 10$ and β-D1D4 $n = 9$. *G*: Relative gene expression levels of insulin gene isoforms in isolated islets; control $n = 10$ and β-D1D4 $n = 6$. Gene expressions were normalized to the housekeeping genes *Sdha* and *Ubc*. *H*: Insulin secretion assay in isolated islets under several stimulants and 10 μmol/L norepinephrine or 10 μmol/L ESI-09; $n = 4$. Male mice 8–10 weeks old were used in the study. Data for *C* and *D* are shown as mean ± SEM; all other data are shown as mean ± SD. Differences were considered statistically significant at $P < 0.05$ using a two-way ANOVA with Bonferroni post hoc test and a two-tailed Student *t* test (*$P < 0.05$, **$P < 0.01$, ***$P < 0.001$, ****$P < 0.0001$).

accounted for hyperglucagonemia in β-D1D4 mice, we stained pancreatic sections with MAFB and glucagon as markers of mature α-cells. We observed a significant increase in both MAFB-positive cells and *Mafb* gene expression in β-D1D4 mice (Fig. 4*G–I*). Moreover, we found an increase in Ki-67 expression in glucagon-positive cells as well as increased glucagon gene expression in islets of β-D1D4 mice, indicating higher proliferation of α-cells in these mice compared with their wild-type littermates (Fig. 4*J–L*).

Next, we examined whether the increase in glucagon-positive α-cells in β-D1D4 mice was of β-cell origin, since the knockout of Delta ligand genes is specific to these cells due to CRE expression driven by the *Pdx1* promoter. Therefore, we stained pancreatic sections of mice for CRE and glucagon. As seen in Fig. 4*M*, we found CRE expression in the cytoplasm of β-cells in both groups before tamoxifen treatment (top panel) and nuclear expression 2 weeks after treatment (bottom panel) in glucagon-negative cells. Additionally, we did not find PDX1-positive cells expressing

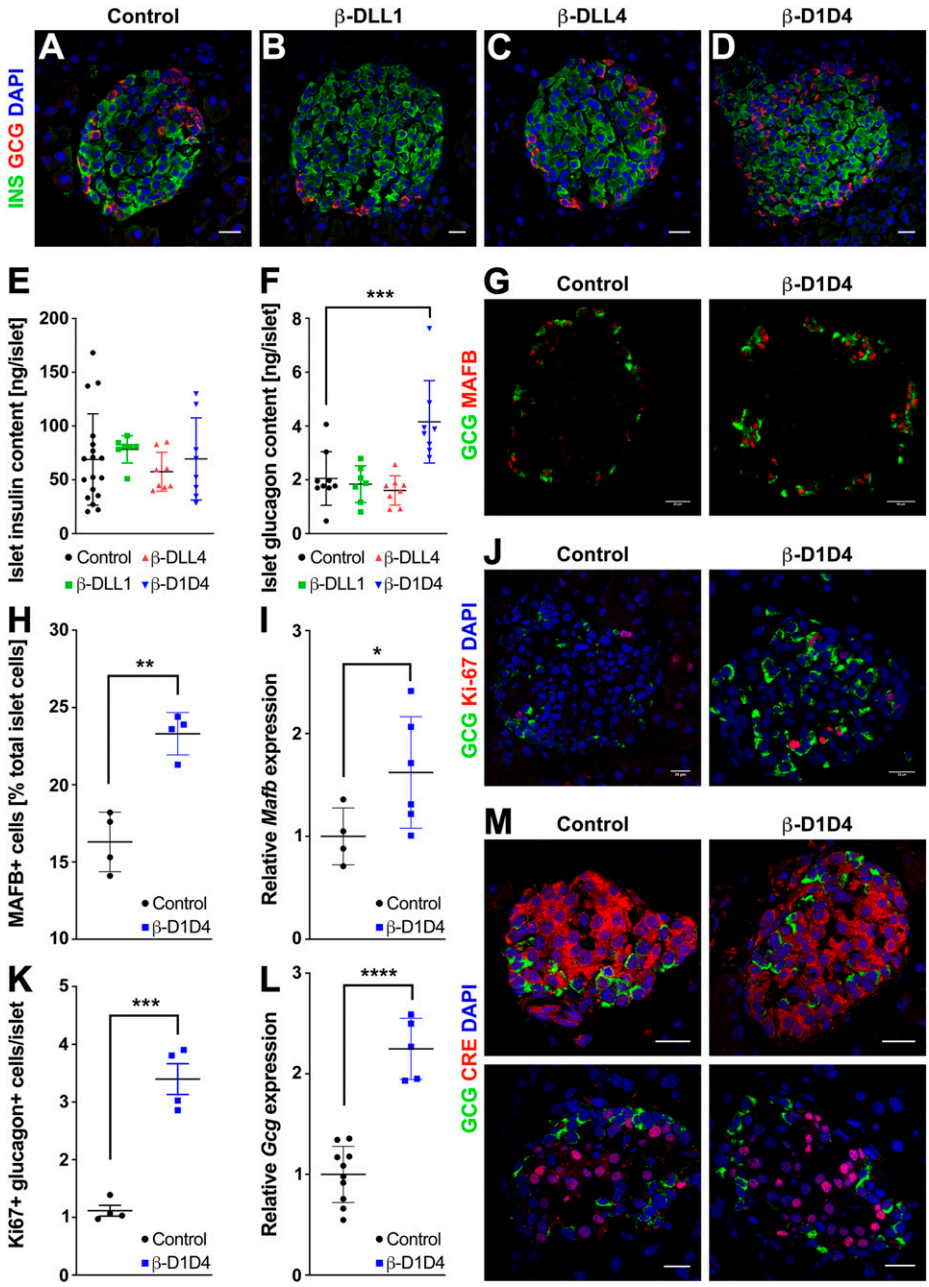

Figure 4—Islet integrity and hormone levels in β-DLL1, β-DLL4, and β-D1D4 mice. Immunostaining for insulin and glucagon in pancreatic sections is shown. *A*: Control mice. *B*: β-DLL1 mice. *C*: β-DLL4 mice. *D*: β-D1D4 mice. $n = 4$. *E*: Concentration of insulin in isolated islets from mutant and control mice. *F*: Concentration of glucagon in isolated islets from mutant and control mice; control $n = 18$, β-DLL1 $n = 7$, and β-DLL4 and β-D1D4 $n = 8$. *G*: Immunostaining for glucagon and MAFB in pancreatic sections of β-D1D4 and control mice. *H*: Quantification of MAFB$^+$ cells; 25–30 islets per genotype; $n = 4$. *I*: Relative gene expression of *Mafb*; control $n = 4$ and β-D1D4 $n = 6$. *J*: Immunostaining for glucagon- and Ki-67–positive islet cells. *K*: Quantification of glucagon- and Ki-67–positive islet cells; $n = 4$. *L*: Relative gene expression levels of glucagon in isolated islets; control $n = 10$ and β-D1D4 $n = 5$. Gene expressions were normalized to the housekeeping genes *Sdha* and *Ubc*. *M*: Immunostaining for glucagon and CRE before (week 0, top panels) and after (week 2, bottom panels) tamoxifen treatment; $n = 4$–5. Eight-week-old male mice were used in the study. Data are shown as mean ± SD. Differences were considered statistically significant at $P < 0.05$ using a one-way ANOVA with Bonferroni post hoc test and a two-tailed Student *t* test (*$P < 0.05$, **$P < 0.01$, ***$P < 0.001$, ****$P < 0.0001$).

glucagon in β-D1D4 mice after tamoxifen treatment (Supplementary Fig. 5*G*). Taken together, the β-cell–specific deletion of both *Dll1* and *Dll4* in adult mice suggests autocrine effects causing increased glucose disposal due to increased insulin secretion and paracrine effects on neighboring non-β-cells.

The DLL1 Intracellular Domain Is Required for Normal Glucose Homeostasis

Previously, it was shown in *Drosophila* that Delta ligands lacking the intracellular domain were able to bind NOTCH but not to activate the pathway, strongly indicating an important functional role (29). Furthermore, in vitro studies

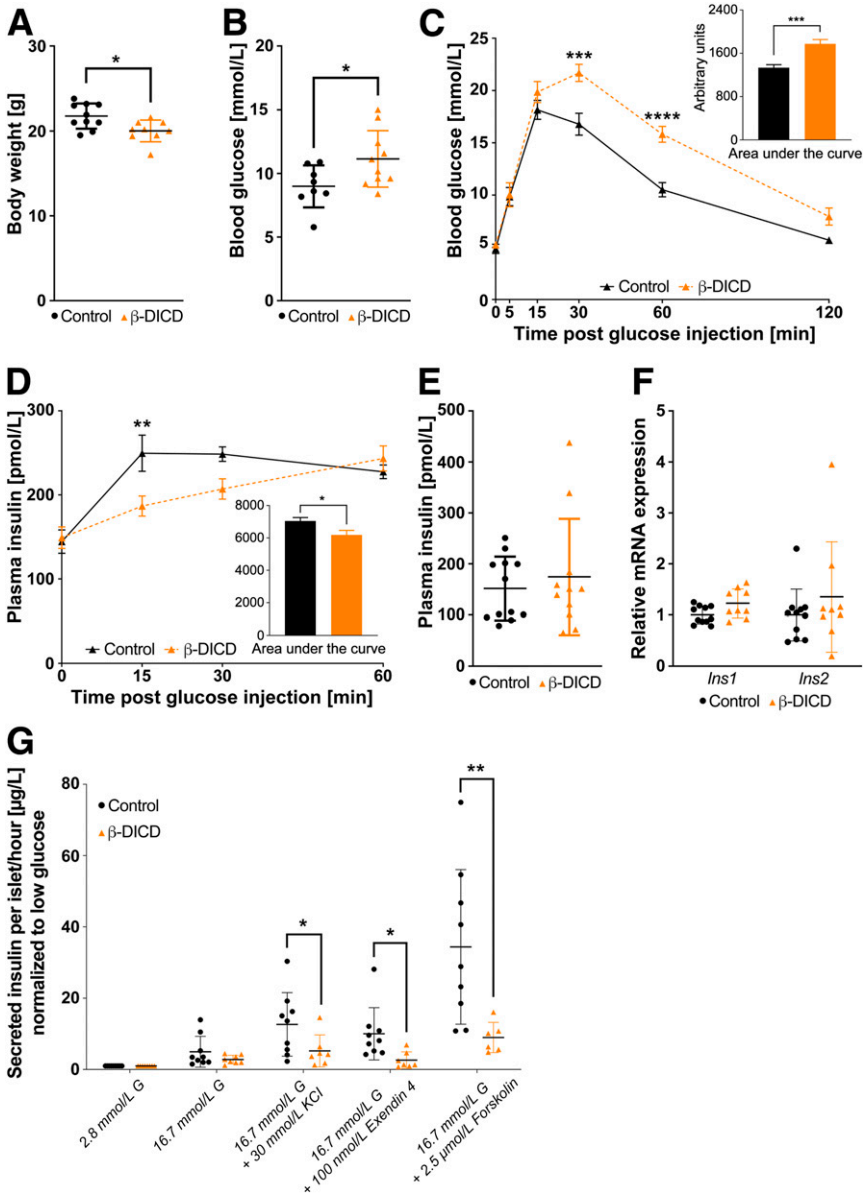

Figure 5—Glucose homeostasis in β-DICD mice. *A*: Average ad libitum fed body weight; control $n = 10$ and β-DICD $n = 9$. *B*: Blood glucose levels of mice; control $n = 8$ and β-DICD $n = 10$. *C*: Measurement of blood glucose levels during an IPGTT. *D*: Measurement of insulin during an IPGTT; control $n = 8$ and β-DICD $n = 9$. *E*: Plasma insulin levels in ad libitum fed state; control $n = 12$ and β-DICD $n = 11$. *F*: Relative gene expression levels of insulin in isolated islets; control $n = 11$ and β-DICD $n = 9$. Gene expressions were normalized to the housekeeping genes *Sdha* and *Ubc*. *G*: Insulin secretion assay in isolated islets; control $n = 9$ and β-DICD $n = 6$. Eight-week-old male mice were used in the study. Data for *C* and *D* are shown as mean ± SEM; all other data are shown as mean ± SD. Differences were considered statistically significant at $P < 0.05$ using a two-way ANOVA with Bonferroni post hoc test and a two-tailed Student *t* test (*$P < 0.05$, **$P < 0.01$, ***$P < 0.001$, ****$P < 0.0001$).

showed that the DICD regulates nuclear signaling by binding to Notch-intracellular domain (30), whereas in the cytoplasm it interacts with components of the transforming growth factor (TGF)-β/activin cascade (31). To analyze the role of the DICD in the adult pancreas, we established a mouse model that conditionally overexpresses the DICD (referred to here as β-DICD) (Supplementary Fig. 1*A* and *B*). To search for possible influences of DICD overexpression on embryonic development, Rosa26-DICD mice were mated to EIIa-cre transgenic mice (32). In agreement with previous findings (14), the analysis of homozygous F2 animals during embryonic development did not reveal any obvious phenotype (data not shown). Successful recombination and DICD overexpression after tamoxifen induction was confirmed on the DNA, mRNA, and protein levels (Supplementary Fig. 1*C*–*E*).

We analyzed male β-DICD mice in vivo and in vitro at 8 weeks of age. The ad libitum fed body weight of β-DICD mice was significantly reduced and blood glucose levels were slightly but significantly increased (Fig. 5*A* and *B*)

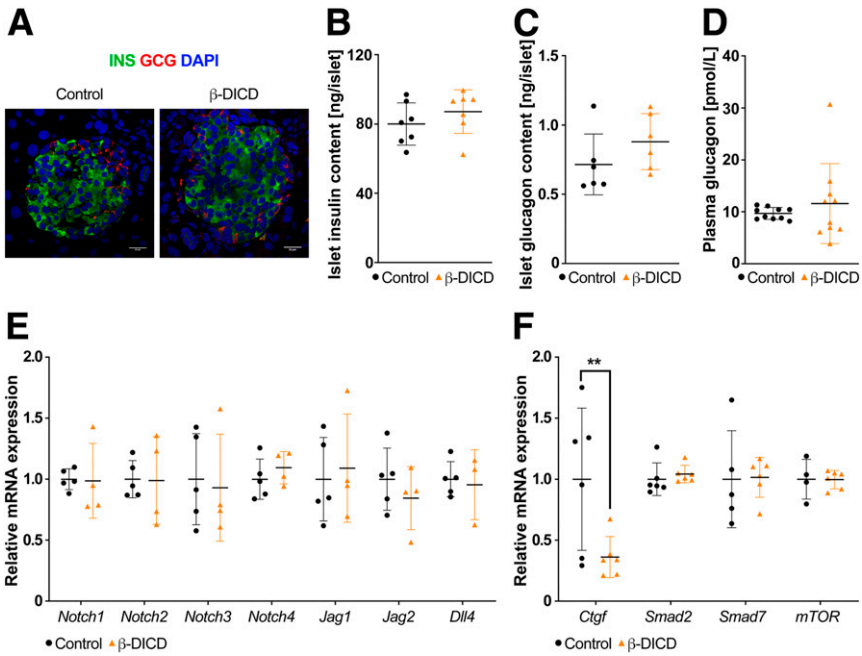

Figure 6— Islet integrity and hormone levels in β-DICD mice. *A*: Immunostaining for insulin and glucagon in pancreatic sections; $n = 4$–5. The scale bar represents 50 μm. *B*: Concentration of insulin in isolated islets; $n = 7$. *C*: Concentration of glucagon in isolated islets; $n = 6$. *D*: Concentration of glucagon in plasma; $n = 10$. *E* and *F*: Relative mRNA expression of D/N components and *Ctgf* as well as TGF-β pathway components in isolated islets; control $n = 5$ and β-DICD $n = 4$ (for *Dll4* $n = 3$). Gene expressions were normalized to the housekeeping genes *Sdha* and *Ubc*. Eight-week-old male mice were used in the study. Data are shown as mean ± SD. Differences were considered statistically significant at $P < 0.05$ using a two-tailed Student *t* test (**$P < 0.01$).

compared with Cre^+ controls. During an IPGTT, β-DICD mice showed a significant delay in glucose disposal compared with controls (Fig. 5*C*). Accordingly, a significantly lower amount of secreted insulin was observed (Fig. 5*D*). However, β-DICD mice showed no significant change in ad libitum fed plasma insulin levels (Fig. 5*E*) or insulin gene expression in isolated islets (Fig. 5*F*). Glucose-stimulated insulin secretion analysis in isolated islets under low-glucose conditions revealed no difference between β-DICD and control mice and only a slight but nonsignificant reduction in insulin secretion under high-glucose conditions. However, additional stimulation with exendin-4 and forskolin revealed that significantly less insulin was secreted by β-DICD, again hinting at a possible connection of DLL1 with adenylyl cyclase (Fig. 5*G*).

Reduced Insulin Secretion in β-DICD Mice Is Independent of Islet Architecture

Next, we wondered whether overexpression of DICD has any effect on islet morphology and β-cell proliferation and maturity. Comparison of islets from 8-week-old male β-DICD mice with Cre^+ controls revealed no obvious differences in their architecture and expression of insulin and glucagon (Fig. 6*A*). Accordingly, insulin and glucagon content per islet was comparable between the groups (Fig. 6*B* and *C*). Furthermore, no change in plasma glucagon was found in β-DICD islets (Fig. 6*D*). In agreement with this finding and the reported transcriptional activity of DICD (30), relative gene expression levels of *Notch1, Notch2, Notch3, Notch4, Dll4*, *Jag1*, and *Jag2* were unaltered in β-DICD compared with control islets (Fig. 6*E*).

Previously, connective tissue growth factor (*Ctgf*), an intermediate of the TGF-β pathway, was found to be associated with DICD (33). Interestingly, although we found a strong downregulation of *Ctgf* in β-DICD islets, other genes with associated TGF-β signaling (*Smad2*, *Smad7*, and *Mtor*) were not altered compared with control islets (Fig. 6*F*). In summary, the β-cell–specific overexpression of DICD does not affect islet morphology, islet hormonal content, and gene expression of D/N pathway intermediates, but it results in a specific insulin secretion defect.

DISCUSSION

In this study, we confirmed the presence of several mediators of the D/N pathway and several features of its components in adult pancreatic islets. Whereas NOTCH2 and NOTCH4 are expressed in some islet cells that, in turn, indicate heterogeneity in the expression of these proteins, NOTCH3 seems to be expressed in the vasculature, indicating a role in the maintenance of blood vessel integrity (34). Consistent with a recent study (8), NOTCH1 was found within the whole adult pancreas, including the presence of activated NOTCH1 within the islet nuclei. Moreover, JAGGED1 is specifically expressed in α-cells, indicating the presence of an active NOTCH-JAGGED signaling pathway. Finally, DLL1 and DLL4 are highly expressed in β-cells, indicating divergence in the expression pattern of Notch ligands in the adult pancreas and, therefore, strongly

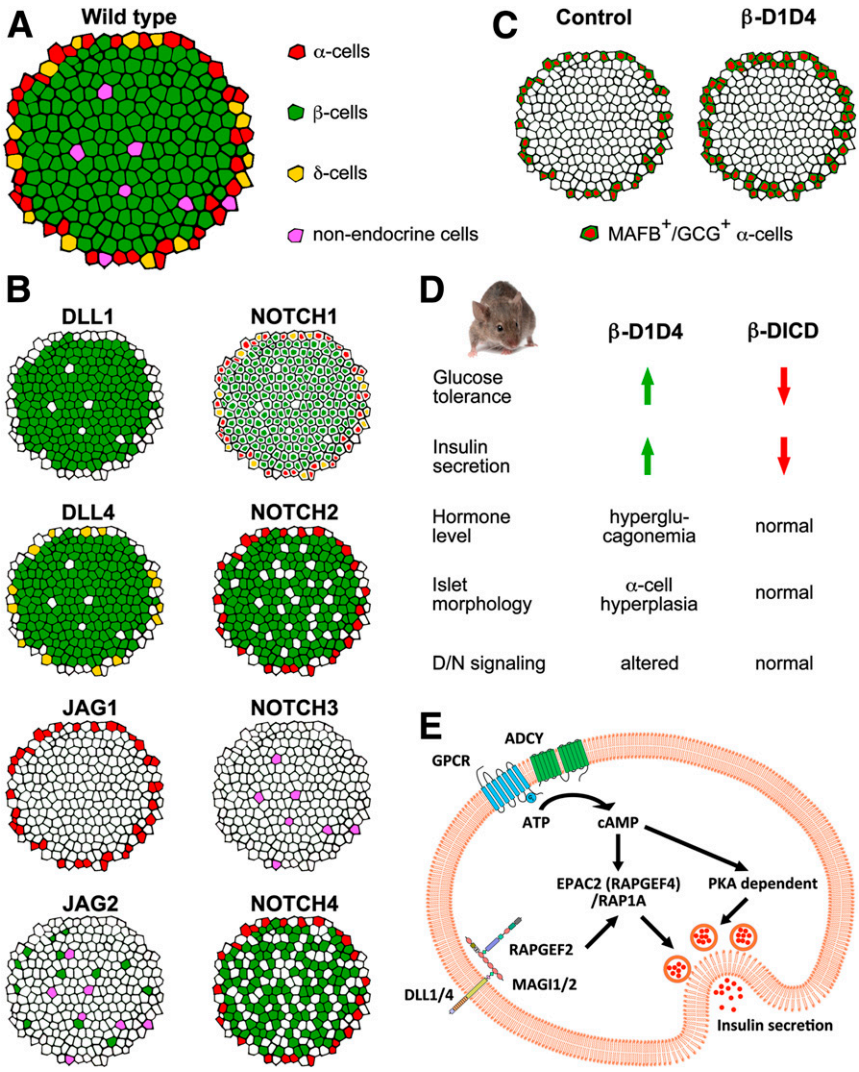

Figure 7—Graphical summary. *A*: Healthy pancreatic islet cell constituents. *B*: Cell-specific protein expression of D/N components within the wild-type islet, depicting α-cells (red), β-cells (green), δ-cells (yellow), nonendocrine cells (purple), and unlabeled cells (white). *C*: A comparative illustration of a control vs. β-D1D4 islets. *D*: A summary of the major phenotypic findings of the β-D1D4 and β-DICD mouse models. *E*: A schematic diagram of the proposed DLL1/4-mediated influence on insulin secretion: RAP1A signaling is amplified by RAPGEF2, a factor that binds to MAGI proteins, which, in turn, can interact with the intracellular domains of DLL1 and DLL4. Differing expressions levels of these intracellular domains might have consequences for EPAC2/RAP1A-associated insulin secretion. PKA, cAMP-dependent protein kinase.

suggesting a novel functional role. In light of these results, we used β-cell–specific knockouts of DLL1 and DLL4 to examine the potential roles of Delta ligands in the homeostasis of adult islets and to provide further evidence of bidirectional D/N signaling by demonstrating the importance of DICD in β-cell function.

A recent study demonstrated that the loss of *Notch1* in adult β-cells protects mice from developing glucose intolerance as a consequence of diet-induced obesity (8). Therefore, the loss of NOTCH1 signaling in adult mouse β-cells leads to a better metabolic profile (8), a feature similar to the concomitant loss of *Dll1* and *Dll4* shown in the current study. However, β-DLL1 mice displayed mild hyperglycemia and impaired glucose tolerance without any observable changes in β- and α-cell masses, and although β-DLL4 mice displayed normoglycemia, in vivo glucose tolerance in β-DLL4 mice was mildly but significantly improved. This was accentuated by the simultaneous loss of both Delta ligands, where a dramatic improvement in glucose tolerance was observed that mimicked loss of NOTCH1 in β-cells (8). The phenotypic discrepancy between β-DLL1 and β-DLL4 mice is rather puzzling, but we speculate that the differences arise due to the divergence in downstream targets upon Notch receptor activation by either DLL1 or DLL4, which are well documented across species and different organ systems (35–37). Moreover, NOTCH1 has been shown to have intrinsic in vitro selectivity for DLL4 over DLL1 (38). However, NOTCH1 activation by either of the Delta ligands is also organ and cell type specific (6,39), and

in the case of murine β-cells, loss of NOTCH1 signaling phenotypically mimics the loss of DLL4 somewhat, thereby presenting DLL4 as the major D/N player in the context of adult β-cell homeostasis.

Interestingly, a recent study used anti-DLL4 antibody administration in mice and reported an increase in insulin production by blocking the DLL4 protein, possibly as a consequence of increased β-cell proliferation (9). Moreover, upregulation of NOTCH1 in β-cells leads to increased proliferation of these cells (8). Therefore, it seems that the two scenarios, loss of Delta ligands and loss of Notch receptors, do not display entirely similar phenotypes. This indicates that despite the loss of Delta ligands, Notch receptor signaling may still be activated. Billiard et al. (9) did not further investigate the state of Notch, but we observed an increase in transcripts of Notch receptors in β-D1D4 mice, including that of the downstream target *Hes1*. Hence, it is likely that Notch signaling is activated by other ligands from neighboring cells when expressions of Delta ligands are downregulated. Here, we showed that JAG1 is specifically expressed in α-cells. We speculate that JAG1 activates Notch signaling in islets of β-D1D4 mice. Indeed, we observed an increase in α-cell proliferation and glucagon levels, along with increased expression of the α-cell maturity marker *Mafb* and of *Jag1*. This, however, will require molecular investigation for further confirmation.

Interestingly, β-DLL1 mice, in which the DICD is also deleted, display mildly increased ad libitum fed blood glucose levels. However, overexpression of the DICD in mice also led to higher blood glucose levels. This discrepancy is likely explained by an effect of the DICD on insulin secretion independently of the D/N pathway, whereas knocking down *Dll1* likely dampens paracrine signaling with regard to DLL1-NOTCH in the β-cells. Therefore, effects associated with overexpression of the DICD must arise from within the cell. In this regard, a study on DICD revealed an association with the TGF-β pathway and *Ctgf* (33), which has been shown to be required for β-cell maturity and proliferation in islets (40,41). In fact, we observed a significant downregulation of *Ctgf* in β-DICD mice. However, the study by Riley et al. (41) was performed after partial β-cell destruction and under nonstimulatory conditions, and no changes in maturity and proliferation of β-cells were observed.

Previously, studies have confirmed the binding of DLL1 and DLL4 intracellular domains to PDZ domain–containing MAGUK proteins such as MAGI1 and 2 (12,42,43). Interestingly, both MAGI1 and 2 bind to RAPGEF2, a guanine nucleotide exchange factor for the small guanosine triphosphatase RAP1A (44,45). Furthermore, components of the GEF family are critical for K_{ATP}- and Ca^{2+} channel-dependent insulin secretion (46), and RAP1A interaction with EPAC2 (RAPGEF4) (47) is essential for first-phase insulin secretion (48). Considering that EPAC2 is one of two pathways downstream of adenylyl cyclase (49,50), it is tempting to speculate that manipulation of DICD expression might have consequences for the availability of MAGI proteins to interact with RAPGEF2 and, in turn, affect its interaction with EPAC2/RAP1A-associated insulin secretion. Several lines of evidence are presented in support of this possibility. First, although some downstream defects might be present, since only a modest increase in insulin secretion was observed upon KCl stimulation, it is upon forskolin stimulation that a lack of considerable potentiation in β-DICD is revealed. Second, a significant increase in insulin secretion was observed with forskolin in β-D1D4 islets. Finally, this significant increase in insulin secretion in β-D1D4 islets can be normalized by inhibiting adenylyl cyclase with norepinephrine and inhibiting EPAC2 by ESI-09. A graphical summary and schematic diagram of the proposed mechanism for the DLL1/4-mediated influence on insulin secretion is given in Fig. 7*E*.

Acknowledgments. The authors thank Freddy Radtke (École Polytechnique Fédérale de Lausanne, Lausanne, Switzerland) for providing us with floxed *Dll1* and *Dll4* Sv/129.C57BL/6 × C57BL/6J mice. Pdx1-Cre^{ERT} mice were a kind gift of Maureen Gannon (Vanderbilt University Medical Center, Nashville, TN). DICD rat monoclonal antibody was provided by Dr. Elisabeth Kremmer (Monoclonal Antibody Core Facility, Helmholtz Zentrum München, Neuherberg, Germany). The authors thank Anna-Lena Amend, Sandra Hoffman, Andreas Mayer, and Michael Schulz (Institute of Experimental Genetics and German Mouse Clinic, Helmholtz Zentrum München, Neuherberg, Germany) for providing excellent technical assistance.

Funding. This work was funded by the German Federal Ministry of Education and Research to the German Center for Diabetes Research.

Duality of Interest. No potential conflicts of interest relevant to this article were reported.

Author Contributions. M.R. designed the study, carried out the research, collected and analyzed the data, and wrote the manuscript. N.F.C. performed experiments, analyzed and interpreted the results, and wrote the manuscript. D.G. generated the β-DICD mouse line, and A.S.-M. carried out experiments. H.L., G.K.H.P., and M.H.d.A. conceived and designed the study, contributed to the interpretation of results, and critically reviewed the manuscript. All authors approved the final version of the manuscript. G.K.H.P. and M.H.d.A. are the guarantors of this work and, as such, had full access to all the data in the study and take responsibility for the integrity of the data and the accuracy of the data analysis.

Prior Presentation. Parts of this study were presented in poster form at The Allied Genetics Conference 2016, Orlando, FL, 13–17 July 2016, and at the 52nd Annual Meeting of the European Association for the Study of Diabetes, Munich, Germany, 12–16 September 2016.

References

1. International Diabetes Federation. *IDF Diabetes Atlas*. 8th ed. Brussels, Belgium, International Diabetes Federation, 2017

2. Ashcroft FM, Rorsman P. Diabetes mellitus and the β cell: the last ten years. Cell 2012;148:1160–1171

3. Morris AP, Voight BF, Teslovich TM, et al.; Wellcome Trust Case Control Consortium; Meta-Analyses of Glucose and Insulin-related traits Consortium (MAGIC) Investigators; Genetic Investigation of ANthropometric Traits (GIANT) Consortium; Asian Genetic Epidemiology Network–Type 2 Diabetes (AGEN-T2D) Consortium; South Asian Type 2 Diabetes (SAT2D) Consortium; DIAbetes Genetics Replication And Meta-analysis (DIAGRAM) Consortium. Large-scale association analysis provides insights into the genetic architecture and pathophysiology of type 2 diabetes. Nat Genet 2012;44:981–990

4. Lai EC. Notch signaling: control of cell communication and cell fate. Development 2004;131:965–973

5. Apelqvist A, Li H, Sommer L, et al. Notch signalling controls pancreatic cell differentiation. Nature 1999;400:877–881
6. Pellegrinet L, Rodilla V, Liu Z, et al. Dll1- and dll4-mediated notch signaling are required for homeostasis of intestinal stem cells. Gastroenterology 2011;140: 1230–1240
7. Dror V, Nguyen V, Walia P, Kalynyak TB, Hill JA, Johnson JD. Notch signalling suppresses apoptosis in adult human and mouse pancreatic islet cells. Diabetologia 2007;50:2504–2515
8. Bartolome A, Zhu C, Sussel L, Pajvani UB. Notch signaling dynamically regulates adult β cell proliferation and maturity. J Clin Invest 2019;129:268–280
9. Billiard F, Karaliota S, Wang B, et al. Delta-like ligand-4-notch signaling inhibition regulates pancreatic islet function and insulin secretion. Cell Rep 2018; 22:895–904
10. Ehebauer M, Hayward P, Martinez-Arias A. Notch signaling pathway. Sci STKE 2006;2006:cm7
11. Bray SJ. Notch signalling: a simple pathway becomes complex. Nat Rev Mol Cell Biol 2006;7:678–689
12. Six EM, Ndiaye D, Sauer G, et al. The notch ligand Delta1 recruits Dlg1 at cell-cell contacts and regulates cell migration. J Biol Chem 2004;279:55818–55826
13. Dyczynska E, Sun D, Yi H, Sehara-Fujisawa A, Blobel CP, Zolkiewska A. Proteolytic processing of delta-like 1 by ADAM proteases. J Biol Chem 2007;282:436–444
14. Redeker C, Schuster-Gossler K, Kremmer E, Gossler A. Normal development in mice over-expressing the intracellular domain of DLL1 argues against reverse signaling by DLL1 in vivo. PLoS One 2013;8:e79050
15. Mishra-Gorur K, Rand MD, Perez-Villamil B, Artavanis-Tsakonas S. Down-regulation of Delta by proteolytic processing. J Cell Biol 2002;159:313–324
16. Remedi MS, Emfinger C. Pancreatic β-cell identity in diabetes. Diabetes Obes Metab 2016;18(Suppl. 1):110–116
17. Hozumi K, Negishi N, Suzuki D, et al. Delta-like 1 is necessary for the generation of marginal zone B cells but not T cells in vivo. Nat Immunol 2004;5:638–644
18. Koch U, Fiorini E, Benedito R, et al. Delta-like 4 is the essential, nonredundant ligand for notch1 during thymic T cell lineage commitment. J Exp Med 2008;205: 2515–2523
19. Zhang H, Fujitani Y, Wright CVE, Gannon M. Efficient recombination in pancreatic islets by a tamoxifen-inducible Cre-recombinase. Genesis 2005;42:210–217
20. Nyabi O, Naessens M, Haigh K, et al. Efficient mouse transgenesis using Gateway-compatible ROSA26 locus targeting vectors and F1 hybrid ES cells. Nucleic Acids Res 2009;37:e55
21. Belteki G, Gertsenstein M, Ow DW, Nagy A. Site-specific cassette exchange and germline transmission with mouse ES cells expressing phiC31 integrase. Nat Biotechnol 2003;21:321–324
22. Chen CM, Krohn J, Bhattacharya S, Davies B. A comparison of exogenous promoter activity at the ROSA26 locus using a ΦiC31 integrase mediated cassette exchange approach in mouse ES cells. PLoS One 2011;6:e23376
23. Li DS, Yuan YH, Tu HJ, Liang QL, Dai LJ. A protocol for islet isolation from mouse pancreas. Nat Protoc 2009;4:1649–1652
24. Bankhead P, Loughrey MB, Fernández JA, et al. QuPath: open source software for digital pathology image analysis. Sci Rep 2017;7:16878
25. Livak KJ, Schmittgen TD. Analysis of relative gene expression data using real-time quantitative PCR and the 2(-Delta Delta C(T)) Method. Methods 2001;25: 402–408
26. Tiano JP, Mauvais-Jarvis F. Importance of oestrogen receptors to preserve functional β-cell mass in diabetes. Nat Rev Endocrinol 2012;8:342–351
27. Straub SG, Sharp GW. Evolving insights regarding mechanisms for the inhibition of insulin release by norepinephrine and heterotrimeric G proteins. Am J Physiol Cell Physiol 2012;302:C1687–C1698
28. Almahariq M, Tsalkova T, Mei FC, et al. A novel EPAC-specific inhibitor suppresses pancreatic cancer cell migration and invasion. Mol Pharmacol 2013; 83:122–128
29. Parks AL, Stout JR, Shepard SB, et al. Structure-function analysis of delta trafficking, receptor binding and signaling in Drosophila. Genetics 2006;174: 1947–1961
30. Jung J, Mo JS, Kim MY, Ann EJ, Yoon JH, Park HS. Regulation of notch1 signaling by Delta-like ligand 1 intracellular domain through physical interaction. Mol Cells 2011;32:161–165
31. Hiratochi M, Nagase H, Kuramochi Y, Koh CS, Ohkawara T, Nakayama K. The Delta intracellular domain mediates TGF-beta/Activin signaling through binding to Smads and has an important bi-directional function in the notch-Delta signaling pathway. Nucleic Acids Res 2007;35:912–922
32. Lakso M, Pichel JG, Gorman JR, et al. Efficient in vivo manipulation of mouse genomic sequences at the zygote stage. Proc Natl Acad Sci U S A 1996;93:5860–5865
33. Bordonaro M, Tewari S, Atamna W, Lazarova DL. The notch ligand Delta-like 1 integrates inputs from TGFbeta/Activin and Wnt pathways. Exp Cell Res 2011; 317:1368–1381
34. Henshall TL, Keller A, He L, et al. Notch3 is necessary for blood vessel integrity in the central nervous system. Arterioscler Thromb Vasc Biol 2015;35: 409–420
35. Nandagopal N, Santat LA, LeBon L, Sprinzak D, Bronner ME, Elowitz MB. Dynamic ligand discrimination in the notch signaling pathway. Cell 2018;172:869–880.e19
36. Mohtashami M, Shah DK, Nakase H, Kianizad K, Petrie HT, Zúñiga-Pflücker JC. Direct comparison of Dll1- and Dll4-mediated notch activation levels shows differential lymphomyeloid lineage commitment outcomes. J Immunol 2010;185: 867–876
37. Preuße K, Tveriakhina L, Schuster-Gossler K, et al. Context-dependent functional divergence of the notch ligands DLL1 and DLL4 in vivo. PLoS Genet 2015;11:e1005328
38. Andrawes MB, Xu X, Liu H, et al. Intrinsic selectivity of notch 1 for delta-like 4 over delta-like 1. J Biol Chem 2013;288:25477–25489
39. Tveriakhina L, Schuster-Gossler K, Jarrett SM, et al. The ectodomains determine ligand function in vivo and selectivity of DLL1 and DLL4 toward NOTCH1 and NOTCH2 in vitro. eLife 2018;e40045
40. Crawford LA, Guney MA, Oh YA, et al. Connective tissue growth factor (CTGF) inactivation leads to defects in islet cell lineage allocation and beta-cell proliferation during embryogenesis. Mol Endocrinol 2009;23:324–336
41. Riley KG, Pasek RC, Maulis MF, et al. Connective tissue growth factor modulates adult β-cell maturity and proliferation to promote β-cell regeneration in mice. Diabetes 2015;64:1284–1298
42. Pfister S, Przemeck GK, Gerber JK, Beckers J, Adamski J, Hrabé de Angelis M. Interaction of the MAGUK family member Acvrinp1 and the cytoplasmic domain of the notch ligand Delta1. J Mol Biol 2003;333:229–235
43. Wright GJ, Leslie JD, Ariza-McNaughton L, Lewis J. Delta proteins and MAGI proteins: an interaction of notch ligands with intracellular scaffolding molecules and its significance for zebrafish development. Development 2004;131:5659–5669
44. Sakurai A, Fukuhara S, Yamagishi A, et al. MAGI-1 is required for Rap1 activation upon cell-cell contact and for enhancement of vascular endothelial cadherin-mediated cell adhesion. Mol Biol Cell 2006;17:966–976
45. Ohtsuka T, Hata Y, Ide N, et al. nRap GEP: a novel neural GDP/GTP exchange protein for rap1 small G protein that interacts with synaptic scaffolding molecule (S-SCAM). Biochem Biophys Res Commun 1999;265:38–44
46. Shibasaki T, Sunaga Y, Seino S. Integration of ATP, cAMP, and Ca2+ signals in insulin granule exocytosis. Diabetes 2004;53(Suppl. 3):S59–S62
47. Liao Y, Kariya K, Hu CD, et al. RA-GEF, a novel Rap1A guanine nucleotide exchange factor containing a Ras/Rap1A-associating domain, is conserved between nematode and humans. J Biol Chem 1999;274:37815–37820
48. Shibasaki T, Takahashi H, Miki T, et al. Essential role of Epac2/Rap1 signaling in regulation of insulin granule dynamics by cAMP. Proc Natl Acad Sci U S A 2007; 104:19333–19338
49. Seino S, Shibasaki T. PKA-dependent and PKA-independent pathways for cAMP-regulated exocytosis. Physiol Rev 2005;85:1303–1342
50. Rutter GA, Pullen TJ, Hodson DJ, Martinez-Sanchez A. Pancreatic β-cell identity, glucose sensing and the control of insulin secretion. Biochem J 2015;466: 203–218